Received: 11 January 2021 | Revised: 26 February 2021 | Accepted: 1 March 2021

DOI: 10.1111/jfpp.15431

ORIGINAL ARTICLE

Journal of Food Processing and Preservation | Institute of Food Science + Technology | ifst | WILEY

Optimization of chestnut starch acetate synthesis by response surface methodology and its effect on dough properties

Na Hu[1] | Luning Li[2]

[1]Asset and Laboratory Management Office, Hebei University of Science and Technology, Shijiazhuang, PR China

[2]Assets Equipment Management Office, Shijiazhuang University, Shijiazhuang, PR China

Correspondence
Luning Li, Assets Equipment Management Office, Shijiazhuang University, Shijiazhuang, 050018, PR China.
Email:

Funding information
the Laboratory Construction and Asset Management Research Project of Higher Education Society, Hebei Province, China, Grant/Award Number: sy202109; the Youth Fund Project of the Education Department, Hebei Province, China, Grant/Award Number: QN2018030

Abstract

Chestnut starch acetate (CSA) was prepared by attaching acetic anhydride groups on chestnut starch (CS) molecules. The process conditions for the preparation of CSA were optimized through single-factor testing and response surface analysis. The optimal conditions were as follows: acetic anhydride content 7%, time of reaction 92 min, temperature 33°C, and pH 8. The actual average apparent viscosity of CSA was 480.53 ± 0.29 mPa·s, which was 109.38% higher than that of natural CS. Fourier transform infrared spectroscopy analysis showed that the hydroxyl group was replaced by the acetyl group on the acetic anhydride. The X-ray diffraction analysis revealed that the crystal form of CSA was type C even after modification. As observed by scanning electron microscopy, the surface of some CSA granules presented different degrees of sag, breakages, and wrinkles. The water retention analysis of the dough revealed that the addition of CSA in the dough was 6%, and the dough had the strongest hydrophilicity and the best water retention. Further, a high number of freeze-thaw cycles reduced the water retention of the dough. The texture characteristics analysis indicated the addition of CSA in the raw dough was 6%–9%, which improved the firmness and toughness of the frozen-thawed dough.

Practical applications

The chestnut processing industry is looking for a new way to develop chestnut derivatives and comprehensively utilize chestnut fruit waste. As the main component of chestnut fruit, starch can be used as a substitute for traditional starch sources such as cereals and tubers. In recent years, modified starch has been widely used in food processing fields such as bread, ice cream, and gluten-free food due to its excellent properties such as high transparency, good stability, and strong water retention. The present study provides an investigation about optimization of chestnut starch acetate (CSA) synthesis by response surface 3D modeling methodology and its effect on dough properties. The results show that the technology of preparing CSA can be regarded as one of the excellent alternative methods to simplify the processing and improve the quality of modified starch. And the modified starch is applied to the dough, the dough shows excellent water retention, and its hardness and toughness are also improved. We believe that the chestnut industry can use the results of this research in the reprocessing of chestnut derivative products and utilization of discarded chestnuts.

1 | INTRODUCTION

Starch acetate is a derivative of starch with a wide range of applications and high commercial value. Starch acetate, in its paste form, has high transparency, high viscosity, more stability, low gelatinization temperature, strong acid and alkali resistance, and excellent freeze-thaw stability compared to starch. Therefore, this product is widely used in food, paper, textiles, medicine, and other industries (Volket et al., 2010; Zhang et al., 2018). Starch acetate with a low degree of substitution is often used as a thickener, gelling agent, and stabilizer in the food industry (Diop et al., 2011; Lin et al., 2019).

The acetylation modification process and characteristics of some common varieties of starch have been studied (Cuenca et al., 2019). Asima et al. (2017) studied the physicochemical, rheological, and structural characterization of acetylated oat starches. Mi et al. (2014) analyzed the effect of potato starch acetate on the freeze cracking of quick-frozen dumpling skins. Pan et al. (2020) researched preparation of cassava acetylated starch by rolling-assisted method. However, further research is necessary to evaluate the potential uses of other alternative starch sources. The main sources of commercial starch are wheat, potato, corn, cassava, rice, and oat (Colussi et al., 2017; Molavi et al., 2018; Przetaczek-Rożnowska, 2017). Nevertheless, other sources, such as chestnut starch, have also been reported and partially characterized (Hu et al., 2020; Oh et al., 2019; Zhang et al. 2019). At present, the available information about the preparation conditions and characteristics of CSA is very limited.

The world production of chestnut fruit is about 1.26 million tons, of which Chinese chestnut production accounts for more than half of the world's total production, ranking first in the world (Bao et al., 2018; Hao et al., 2018; Tang et al., 2019). The starch content in chestnut fruit is between 50% and 80% (dry weight). This crop can be a good substitute for traditional starch sources such as tubers and cereals (Ahmed & Al-Attar, 2015; Wang et al., 2019). Chestnut fruits are highly perishable and seasonal. Some chestnut fruits are discarded during industrial processing due to their undesirable shape, color, and size, insect bites, plagues, and other deformities. Such discarded fruits account for about 30%; thus, it can be used as a cheap source of starch. This will improve the economic efficiency of the industrial process. Thus, we selected this source of starch to increase the utilization of discarded chestnuts and valorize the waste of the chestnut industry (Fariña et al., 2019; Liu et al., 2015; Zhao et al., 2018). Natural chestnut starch lacks some properties, such as low viscosity and poor freeze-thaw stability, which limit its application in the food industry (Attanasio et al., 2014; Hu et al., 2014; Oh et al., 2017). In order to overcome these limitations, starch can be modified to meet the needs of industrial processes.

In this study, chestnut starch and acetic anhydride were used to prepare chestnut starch acetate (CSA) through wet methods, and the preparation conditions were optimized. This process could be an alternative for the development of chestnut products and effective utilization of waste chestnut fruit.

2 | MATERIALS AND METHODS

2.1 | Materials

Chinese chestnut fruits (*Castanea mollissima* Blume) were harvested in QianXi, Hebei Province, China. Acetic anhydride was purchased from Xilong Chemical Co., Ltd. (Shijiazhuang, China). Other chemicals were of analytical reagent grade (Zhenhua Chemical Reagent Co., Ltd. Shijiazhuang, China).

2.2 | Preparation of CS

CS was prepared according to the method of Hu et al. (2020). The chestnut kernel was peeled and chopped into small pieces and immersed in NaOH solution (0.2%, w/v) for 3 hr at 4°C. Subsequently, CS was obtained as a precipitate in water after grinding, homogenizing, centrifuging, washing, and lyophilizing (at −30°C for 36 hr with the vacuum degree of 0.01 MPa).

2.3 | Preparation of CSA

Starch slurry (40%, w/w) was prepared by adding distilled water to 10 g CS to a final weight of 25 g in a beaker. A desired amount of acetic anhydride was added to the starch slurry, which reacted for a period of time under suitable temperature and pH conditions (0.75 mol/L NaOH to adjust pH). The mixture slurry was stirred by a magnetic stirrer until the reaction was over, and the pH of the reaction system was adjusted to 7 with 0.5 mol/L hydrochloric acid. The reaction product was filtered in a suction filter machine to obtain acetylated starch. The wet starch was eluted three times with distilled water to remove unreacted acetic anhydride; the eluted product was then dried in a freeze-dryer for 24 hr to obtain CSA. The acetylation reaction is shown in Figure 1.

2.4 | Preparation of dough samples

Dough samples were prepared according to the method described by Wang et al. (2017) with slight modifications. The flours were prepared by adding different amounts of CSA (0%, 3%, 6%, 9%, and 12% = percentage of dry basis, w/w). Then flour was mixed with water at a ratio of 2:1 (m/V), the dough was kneaded for 15 min, wrapped with a plastic wrap, and placed at 25°C for 1 hr. The dough was frozen at −20°C for 24, 48, 72, 96, and 120 hr, then thawed at 40°C for 1 hr. The dough samples without CSA and after 1, 2, 3, 4, and 5 freeze-thaw cycles were denoted as F_0, F_1, F_2, F_3, F_4, and F_5, respectively.

2.5 | Experimental design and statistical analysis

In order to determine the effect of the amount of acetic anhydride on the apparent viscosity of starch acetate, the chestnut starch was

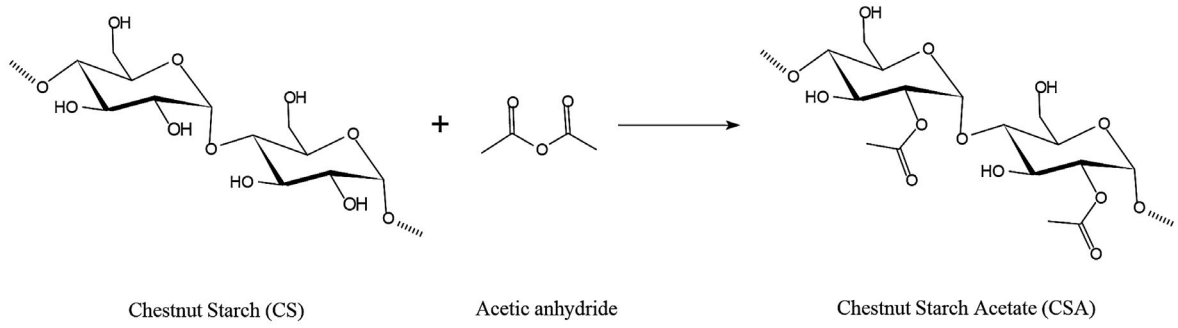

FIGURE 1 The esterification process of chestnut starch by with acetic anhydride

acetylated with different amounts of acetic anhydride (2%, 4%, 6%, 8%, and 10% of dry weight, w/w) at 30°C for 90 min, and pH 8. In order to study the effect of temperature on the apparent viscosity of starch acetate, the chestnut starch was acetylated with 6% acetic anhydride (w/w) at different reaction temperatures (10, 20, 30, 40, and 50°C) for 90 min and pH 8. In order to understand the effect of reaction time on the apparent viscosity of starch acetate, the chestnut starch was acetylated with 6% acetic anhydride (w/w) at 30°C for different reaction time (30, 60, 90, 120, and 150 min) and pH 8. In order to investigate the effect of pH on the apparent viscosity of starch acetate, the chestnut starch was acetylated with 6% acetic anhydride (w/w) at 30°C for 90 min and different pH (7, 8, 9, 10, and 11).

Based on the single-factor test, the appropriate range of each factor was determined, and response surface methodology (RSM) was used to determine optimum conditions. As shown in Table 1, the four factors chosen for this study were designated as X_1, X_2, X_3, and X_4. These factors are divided into three levels, coded as −1, 0, and +1 for low, medium, and high values, respectively. The apparent viscosity of the sample was taken as the response value.

Based on the experimental data, a second-order polynomial model corresponding to the center group and design of the response surface was fitted to predict the optimal conditions. The nonlinear second-order polynomial model is expressed as follows:

$$V = \beta_0 + \sum_{i=0}^{4} \beta_i X_i + \sum_{j=0}^{4} \beta_{ii} X_i^2 + \sum_{i=0}^{4} \sum_{j=0}^{4} \beta_{ii} X_i X_j$$

where V is the response function. β_0 is a constant; Xi is the coded level of independent variables. X_i^2 and X_iX_j present the quadratic and interaction terms, respectively. β_{ii}, β_{ij}, β_i are the quadratic, interactive, and linear coefficients, respectively.

2.6 | Analysis of apparent viscosity

The apparent viscosity of the CS sample was determined using the method described by Hu et al. (2014).

2.7 | Structural characteristics of CS samples

2.7.1 | FTIR spectroscopy

FTIR spectra of CS and modified CS were recorded on Nicolet 8700 FFTIR spectrometer (Thermo Fisher Scientific, Waltham, MA, USA). All spectra were obtained from 400 to 4,000 cm^{-1} at a resolution of 4 cm^{-1} (Sukhija et al., 2016).

2.7.2 | Crystal analysis

The crystalline properties of CS and CSA were analyzed using D8 ADVANCE X-ray diffractometer (Bruker Co., Ltd., Karlsruhe, Germany). The scanning region of diffraction angle ranged from 1.5° to 60° (2θ) with a scanning speed of 8°(2θ)/min (Jeddou et al., 2016).

2.7.3 | SEM analysis

The granules of CS and CSA were examined by S-4800I SEM instrument (Hitachi Company, Tokyo, Japan). The samples were scanned and photographed under the conditions of electron gun acceleration of 20 KV and magnification of 1,000, 3,000, and 5,000 according to the method of Zhang et al. (2018).

2.8 | Analysis of water retention of dough samples

Syneresis is generally used to indicate the water retention of the sample. The higher syneresis, the weaker the water retention, and vice versa.

$$\text{Syneresis}(\%) = (\text{Weight of dough} - \text{weight of dough after freezing and thawing}) / \text{weight of dough} \times 100$$

2.9 | Texture characteristics of raw dough

The dough was pressed to a thickness of 4 mm, cut into a circular piece with a 45-mm circular mold. The firmness and toughness of the

TABLE 1 Box-Behnken experimental design with four independent variables and results

		Levels		
Coded symbols	**Factors**	**−1**	**0**	**1**
X_1	Amount of acetic anhydride (%)	5	6	7
X_2	Time (min)	70	90	110
X_3	Temperature (°C)	25	30	35
X_4	pH	7.5	8.0	8.5

	Independent variables				Responses
Run	**Amount of acetic anhydride (%)**	**Time (min)**	**Time (°C)**	**pH**	**Apparent viscosity (mPa·s)**
1	6	90	25	7.5	411.12
2	7	90	30	7.5	433.55
3	7	70	30	8.0	448.51
4	6	90	35	7.5	433.54
5	6	70	30	7.5	410.98
6	6	90	30	8.0	470.33
7	6	90	30	8.0	465.13
8	7	90	35	8.0	457.65
9	6	70	25	8.0	418.69
10	6	110	30	8.5	455.98
11	6	70	30	8.5	455.97
12	6	110	30	7.5	441.02
13	5	90	25	8.0	411.12
14	7	90	30	8.5	470.92
15	6	110	25	8.0	433.55
16	7	90	25	8.0	418.61
17	6	90	35	8.5	470.92
18	5	70	30	8.0	426.07
19	5	90	30	7.5	421.03
20	6	90	25	8.5	426.07
21	6	90	30	8.0	478.44
22	5	90	35	8.0	426.07
23	1	110	30	8.0	463.45
24	5	90	30	8.5	426.07
25	5	110	30	8.0	426.23
26	6	70	35	8.0	448.51
27	6	90	30	8.0	470.94
28	6	90	30	8.0	461.22
29	6	110	35	8.0	455.98

dough were measured by a Universal TA texture analyzer (Shanghai Tengba Instrument Technology Co., Ltd., Shanghai, China). The test probe used P/BS probe and the pretest speed was 2 mm/s, the measurement speed was 2 mm/s, the post-test speed was 2 mm/s. The compression distance was 30 mm, the trigger force was 10 g, the compression rate was 70%, the test interval was 4 s, and the trigger force type was automatic.

2.10 | Statistical analysis

The experimental data of dough texture analysis were mean values of six replications ± standard deviation. Other experimental data were the average of triplicate experiments, which were expressed as mean ± standard deviation. The data were analyzed using SPSS 19.0 software. The design-expert 8.0.6 (Stat-Ease Inc., Minneapolis, MN)

was used for the experimental design and regression analysis of the experimental data.

3 | RESULTS AND DISCUSSIONS

3.1 | Single factor result analysis

3.1.1 | Effect of amount of acetic anhydride on the apparent viscosity of modified starch

Figure 2a indicates that the apparent viscosity of the sample increased significantly as the amount of acetic anhydride increased and reached 414.06 mPa·s at 6%. Then, the apparent viscosity increased slowly. The possible reason for this phenomenon is that in the early stage of the reaction, as the amount of acetic anhydride increased, the probability of collision between the acid anhydride and the active center Starch-O^- Na^+ increased, and the effective collision of the reaction also increased. This significantly increased the degree of starch acetylation and apparent viscosity. Because the starch molecules had already been consumed in large amounts in the early reaction, a further increase in acetic anhydride drastically reduced the pH of the reaction (Lin et al., 2019). Therefore, the chance of hydrolysis of acetic anhydride was increased under acidic conditions, which was not conducive to the reaction. As a result, the reaction efficiency decreased and the apparent viscosity increased slowly.

3.1.2 | Effect of time on the apparent viscosity of modified starch

As can be seen in Figure 2b, the apparent viscosity of CSA increased with the extension of reaction time, reaching the maximum value at 90 min, then the apparent viscosity decreased with further increasing the time. The possible reason is that with the extension of the reaction time, the contact time of the reactants increased, and the starch structure became looser. Meanwhile, the accelerated thermal motion of the molecules was conducive to the contact between the reaction groups, resulting in the complete acetylation reaction, a higher degree of acetylation, and correspondingly higher apparent viscosity (Xiao et al., 2016). After 90 min, the reaction efficiency decreased with the decrease of reactant concentration. Moreover, when the reaction reached equilibrium, the hydrolysis rate of starch acetate was faster than the synthesis rate of starch acetate. In addition, under high-temperature conditions, the acetylation of the reactants reached a certain level, and the reaction time continued to

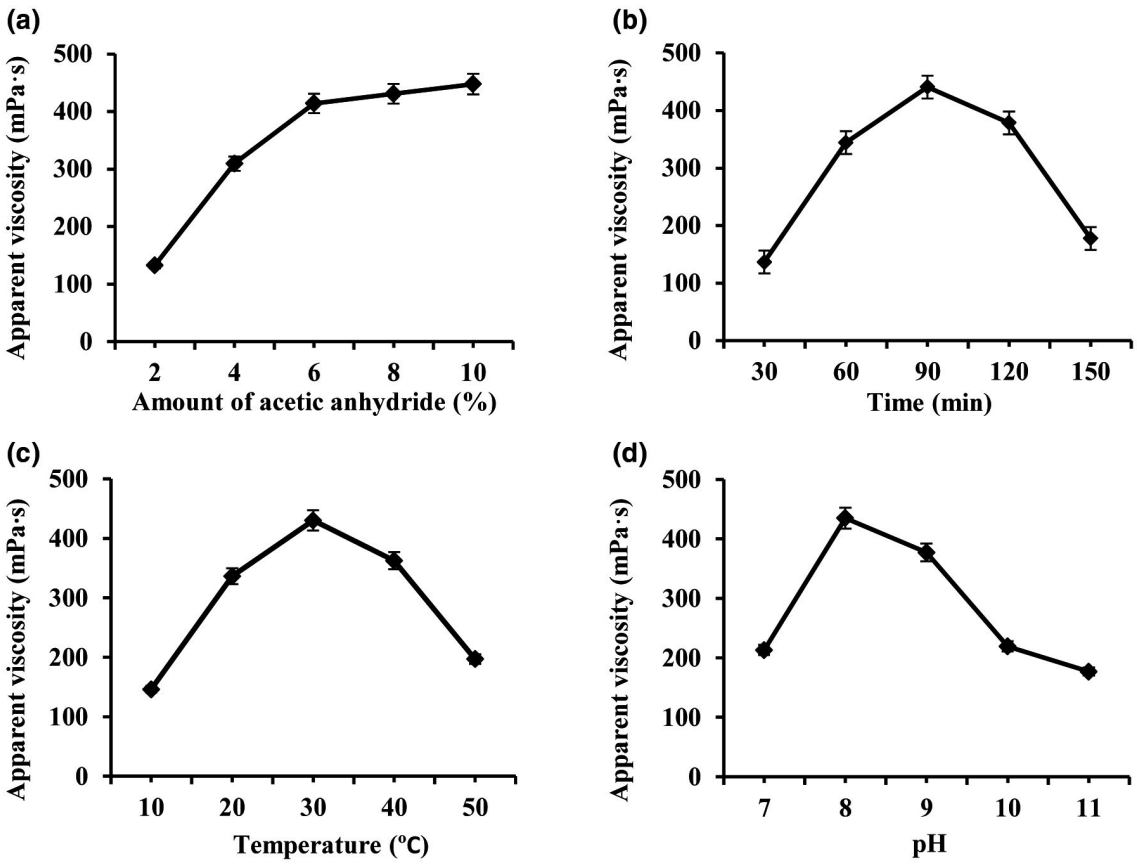

FIGURE 2 The effect of different reaction parameters: (a) amount of acetic anhydride; (b) time; (c) temperature; (d) pH on the apparent viscosity of CSA

be extended, resulting in the degradation and gelatinization of the starch molecules themselves, which reduced the apparent viscosity of the product. Therefore, the appropriate reaction time was 90 min.

3.1.3 | Effect of temperature on the apparent viscosity of modified starch

Figure 2c shows that the apparent viscosity was highest (430.14 mPa·s) at 30°C. This is mainly attributed to the increase in the temperature, which was conducive to the expansion of starch grains. This improved the fluidity of the reagent so that more acetic anhydride molecules reacted with a large number of exposed hydroxyl groups of starch particles. Further, the degree of esterification increased, and the apparent viscosity also increased (Sun et al., 2016). Nevertheless, the reaction temperature was too high, which was not conducive to the adsorption of starch molecules to sodium hydroxide and the formation of the active center Starch-O^- Na^+. Thus, the hydrolysis rate of starch acetate and acetic anhydride increased, which was greater than the esterification rate, resulting in a decrease in the degree of substitution. This, in turn, reduced the apparent viscosity of the CSA. Therefore, the suitable reaction temperature was 30°C.

3.1.4 | Effect of pH on the apparent viscosity of modified starch

CS was acetylated through wet-heating in the presence of acetic anhydride at various pH conditions. Figure 2d shows the change in the apparent viscosity of the modified starch at various conditions. The acetylation of starch was accelerated as the pH was increased from 7 to 8 but diminished at pH > 8. The possible reason is that as the pH value increased, NaOH molecules penetrated into the amorphous region and crystal lattice of the starch granules more quickly, breaking the hydrogen bonds between the starch molecules, causing the lattice spacing to increase, deform, or damage. At this time, the starch granules swelled, and acetic anhydride was more likely to replace the hydrogen on the hydroxyl group of the starch molecule, which increased the degree of substitution, resulting in an increase in apparent viscosity (Cuenca et al., 2019). On the other hand, starch granules were destroyed and gelatinized at a very high pH. Moreover, the modified starch was easily hydrolyzed, and the esterification efficiency was reduced, which reduced the apparent viscosity of CSA. Therefore, the suitable pH of the reaction system was 8.

3.2 | Response surface experiment

3.2.1 | Model fitting and statistical analysis

The preparation process of CSA was optimized according to the Box-Behnken central combination experiment principle. In which, 29 sets of experiments were designed. Multivariate regression fitting was carried out on the experimental data (Table 1), and the dependent variable and the independent variables were related using the following second-order polynomial equation:

$$V = 469.21 + 13.01X_1 + 5.62X_2 + 14.46X_3 + 12.89X_4 + 3.70X_1X_2 + 6.02X_1X_3 + 8.08X_1X_4 - 1.85X_2X_3 - 7.51X_2X_4 + 5.61X_3X_4 - 18.10X_1^2 - 11.14X_2^2 - 20.28X_3^2 - 14.61X_4^2$$

where V is the apparent viscosity; X_1, X_2, X_3, and X_4 are the coded values of amount of acetic anhydride, time, temperature, and pH, respectively.

Table 2 shows the ANOVA results of the response surface model. The statistical significance of the regression equation was verified by F test, and p value was used to determine the significance of each coefficient. The p value of the model was less than .0001, indicating that the model was suitable for this experiment. The determination coefficient (R^2) was 0.9681, which indicated a satisfactory correlation between the predicted and actual values. The adjusted R^2 = 0.9362 indicated that the variation (>93.62%) in apparent viscosity was mostly predicted by the models. The Pred-R^2 of 0.8720 is in reasonable agreement with the Adj-R^2 of 0.9362. The F value of 0.56 implied that the lack of fit was not significant relative to the pure error. Nonsignificant lack of fit was good, which made the model fit desirably. The regression model was determined to be statistically significant at a 95% confidence level. The p value of the models indicated that independent variables (X_1, X_2, X_3, and X_4), interaction terms (X_1X_3, X_1X_4, and X_2X_4), and quadratic terms (X_1^2, X_2^2, X_3^2, and X_4^2) were significant model terms, which dramatically affected apparent viscosity of the modified starch. The acetic anhydride content (X_1), temperature (X_3), and pH (X_4) were the most important factors that affected apparent viscosity of the products, followed by time (X_2), the interaction between acetic anhydride and pH (X_1X_4), the interaction between acetic anhydride and temperature (X_1X_3), and the interaction between time and pH (X_2X_4).

3.2.2 | Response surface analysis and optimization of parameters

The three-dimensional response surface plots between the two factors are shown in Figure 3. They provided a visual interpretation of the interactions between the two factors. The interaction term between acetic anhydride and temperature (X_1X_3) was significant ($p \le .05$), as well as the interaction term between time and pH (X_2X_4). The interaction term between acetic anhydride and pH (X_1X_4) presented high significance ($p \le .01$).

Figure 3a showed that the effects of amount of acetic anhydride and temperature on the apparent viscosity of CSA. At low amount of acetic anhydride levels, temperature had little effect on the apparent viscosity of CSA. As the amount of acetic anhydride increased to 6.1%, the apparent viscosity increased with an increase

TABLE 2 ANOVA for response surface quadratic model

Source	Sum of squares	Degree of freedom	Mean square	*F* value	*p* value (Prob > *F*)
Model	12,378.41	14	884.17	30.35	<.0001**
X_1—Amount of acetic anhydride (%)	2,030.60	1	2,030.60	69.70	<.0001**
X_2—Time (min)	379.46	1	379.46	13.03	.0028**
X_3—Temperature (°C)	2,508.81	1	2,508.81	86.12	<.0001**
X_4—pH	1,994.08	1	1,994.08	68.45	<.0001**
X_1X_2	54.61	1	54.61	1.87	.1925
X_1X_3	145.08	1	145.08	4.98	.0425*
X_1X_4	261.31	1	261.31	8.97	.0096**
X_2X_3	13.65	1	13.65	0.47	.5048
X_2X_4	225.45	1	225.45	7.74	.0147*
X_3X_4	125.78	1	125.78	4.32	.0566
X_1^2	2,124.20	1	2,124.20	72.91	<.0001**
X_2^2	804.81	1	804.81	27.63	.0001**
X_3^2	2,667.14	1	2,667.14	91.55	<.0001**
X_4^2	1,384.59	1	1,384.59	47.53	<.0001**
Lack of fit	237.94	10	23.79	0.56	.7917
Pure error	169.93	4	42.48		
Cor total	12,786.28	28			
R^2	0.9681				
Adj. R^2	0.9362				
Pred. R^2	0.8720				

*Significant ($p \leq .05$); nonsignificant ($p > .05$).

**Highly significant ($p \leq .01$).

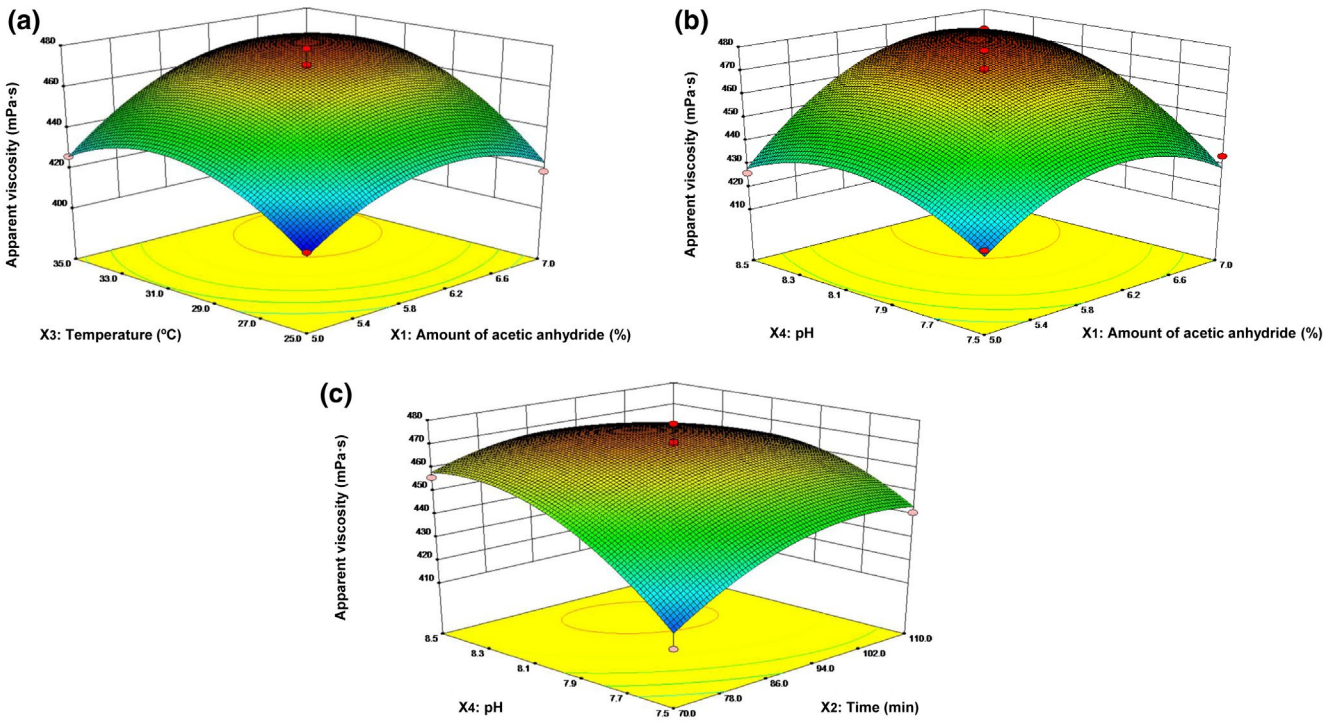

FIGURE 3 The effects of the interaction between two factors (a) amount of acetic anhydride and temperature, (b) amount of acetic anhydride and pH, (c) time, and (d) pH) on the apparent viscosity of CSA

in temperature. Therefore, a slightly higher temperature was required to achieve maximum increase in the apparent viscosity of CSA. Meantime, when the amount of acetic anhydride was increased in the range from 5% to 6.1%, the apparent viscosity of CSA was greatly increased. which indicated that 6.1% concentration of acetic anhydride was required to achieve maximum increase in the apparent viscosity of CSA.

The effects of amount of acetic anhydride and pH on the apparent viscosity of CSA were shown in Figure 3b. An increase in the apparent viscosity of CSA could be significantly achieved with the increases of pH, especially the amount of acetic anhydride increased to 6.1%. Increased pH up to an appropriate threshold led to increasing the apparent viscosity of CSA. Beyond this threshold, the apparent viscosity of CSA slightly decreased. when the pH increased up to about 8, amount of acetic anhydride had an important factor for improving the apparent viscosity yield.

It could be seen from Figure 3c that the effects of time and pH on the apparent viscosity of CSA. The apparent viscosity of CSA mainly depended upon pH and resulted in a curvilinear great increase when pH was increased in the range from 7.5 to 8, and then decreased in the apparent viscosity of CSA. An increase in the apparent viscosity resulted when time was increased in the range from 70 to 90 min, and the time curve started to level off at 90 min, which indicated that 90 min was required to achieve maximum increase.

The purpose of optimization was to determine the conditions of the maximum apparent viscosity of CSA. The optimal values of the factors were obtained by solving the regression equation. The optimal conditions of the factors and the predicted value of apparent viscosity were also given, as shown below: acetic anhydride content 6.61%, time 91.48 min, temperature 32.7°C and pH 8.15, the predicted apparent viscosity of CSA was 481.79 mPa·s. Considering the operability and convenience in actual production, the optimal preparation conditions can be modified as follows (Table 3): acetic anhydride content 7%, time 92 min, temperature 33°C, and pH 8. The actual, apparent viscosity of CSA was 480.53 ± 0.29 mPa·s ($n = 3$), and the relative error between the actual value and the predicted value was 0.26%, indicating that the parameters obtained by the model were reliable and sufficient for acetylation modification.

3.3 | FT-IR analysis

The infrared spectra of native CS and CSA are shown in Figure 4. The characteristic absorption peaks of chestnut starch are mainly attributed to O–H bending, C–H bending, and C–O–C bending (Kamarudin & Gan, 2016; Suvakanta et al., 2014). The absorption peak at 3,400 cm^{-1} is caused by the stretching vibration of the hydroxyl group (O–H). The characteristic absorption peak occurred at 2,930 cm^{-1}, which is ascribed to C–H stretching vibration. The peak at 1,154 cm^{-1} is assigned to C–O–C bonds stretching vibration of glycosidic bond, and the absorption peak at 1,647 cm^{-1} is attributed to the hydroxy stretching vibration of polysaccharides. The new characteristic absorption peak of the CSA at 1,728 cm^{-1} is

TABLE 3 Predicted and experimental values of responses at optimum conditions

Optimum condition				Apparent viscosity (mPa·s)		
Amount of acetic anhydride (%)	Time (min)	Temperature (°C)	pH	Experimental (mPa·s)	Predicted (mPa·s)	Desirability
7	92	33	8	480.53 ± 0.29	481.79	0.80

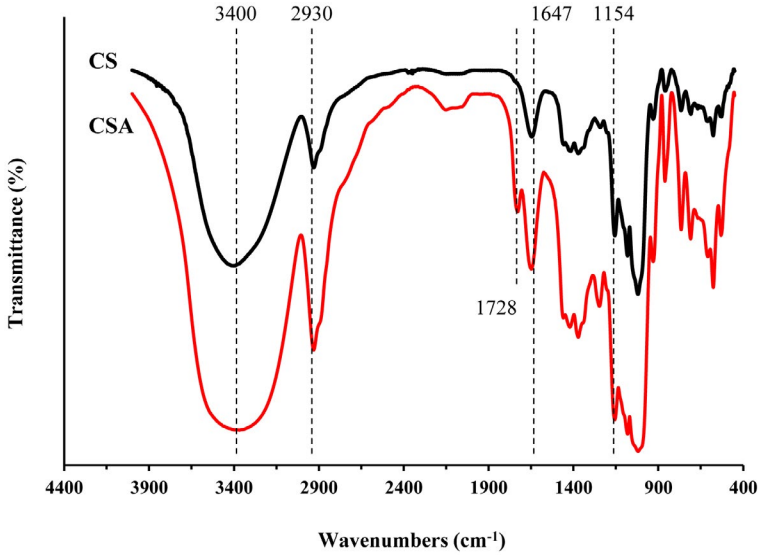

FIGURE 4 FT-IR spectra of CS and CSA

generated by the stretching vibration of the carbonyl group, indicating the presence of C=O, which showed that the acetyl group on the acetic anhydride had replaced the hydrogen on the hydroxyl group of CS molecule, and the characteristic peaks of other groups have not changed significantly (Chylińska et al., 2016; Xu et al., 2010). Therefore, the esterification modification introduced acetyl groups on the original starch molecules.

3.4 | XRD analysis

The crystal structure of starch granules also reflects some differences with plant species from different sources. The crystal structure can be divided into three types, namely, A, B, and C (Liu et al., 2015; Yu et al., 2016). The XRD patterns of the original CS and CSA are presented in Figure 5. CS showed obvious diffraction peaks at 15.3°, 17.3°, and 23.1°, which showed a single peak at 23.1° compared with type B. Therefore, the crystal form of CS was determined as C-type. The characteristic diffraction peaks of CSA appeared at the same position as the original peak of CS; however, the intensity of the peaks was slightly diminished compared with the original starch. It can be seen that the crystal form of CSA was type C even after modification. This indicated that the substitution of acetyl groups for the hydroxyl groups on the starch molecule mainly occurred in the noncrystalline region, which also had some damage to the crystalline region, but the damage of the crystallization region of CS by esterification was insufficient to change the crystal form. Hence, the acetylation modification did not change the crystal type of CS. Therefore, the crystal structure of CSA showed the same trend as shown by the FTIR analysis.

3.5 | SEM analysis

A scanning electron microscope was performed to compare the morphology of CS and CSA granules. Figure 6a,b shows that the surface of the CS granules was smooth, without edges and cracks. The shapes were complex and diverse, usually appeared in ellipses, circles, pears, triangles, and irregular shapes. The surface of CS granules treated with acetic anhydride presented different degrees of depression, breakages, and wrinkles. In addition, some starch granules adhered to each other, whose boundaries were blurred (Figure 6c,d). This may be attributed to the fact that starch granules had a unique layered structure, where the inner layer of the granules was mainly a noncrystalline area with a relatively loose structure, and the outer layer of the granules was a crystalline area with a compact structure. Acetyl groups were introduced into the starch molecules during the acetylation process, which weakened the interlaminar particle binding force of the starch layer, and the amorphous regions were destroyed, resulting in lattice defects, which reduced the crystallinity of starch particles. At the same time, the crystalline area on the surface layer of starch granules also suffered a certain degree of damage, causing the starch granules to stick together and not become independent granules. This conclusion is consistent with the XRD analysis.

3.6 | Water retention analysis

Figure 7 shows syneresis of the dough undergoing different freeze-thaw cycles. With the increase of CSA, the water loss of dough first decreased and then increased. Syneresis was the lowest when the additive amount of CSA was 6%. More freeze-thaw cycles resulted in a higher water loss rate of the dough, resulting in poor water retention. The main reason is that the addition of CSA brought certain hydrophilic groups, which can give the dough good hydrophilicity, promoted the cross-linking of starch molecules, formed a stable gluten network structure, and increased the water retention of the dough (Paulik et al., 2019). However, a high level of modification diluted the protein in the flour (Galvão et al., 2018; Ziobro et al., 2012), inhibiting the formation of gluten and reducing the strength of gluten, which increased water loss. Therefore, the addition of CSA in the dough should not be too high; 6% was an appropriate amount.

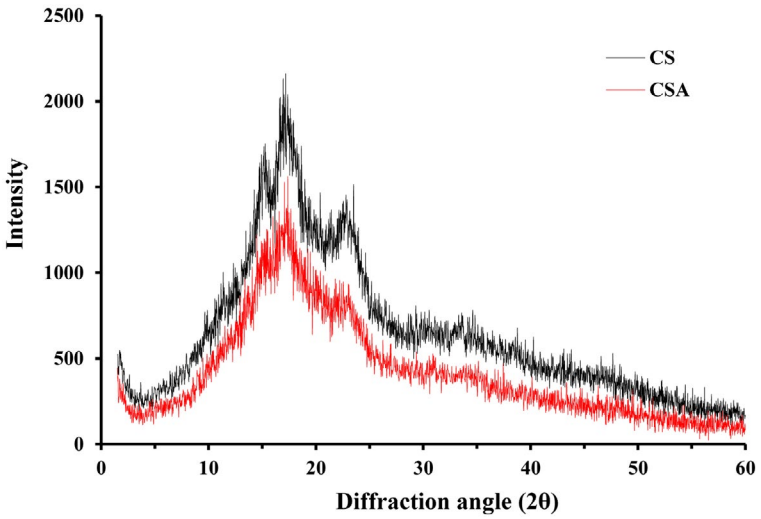

FIGURE 5 XRD analysis of CS and CSA

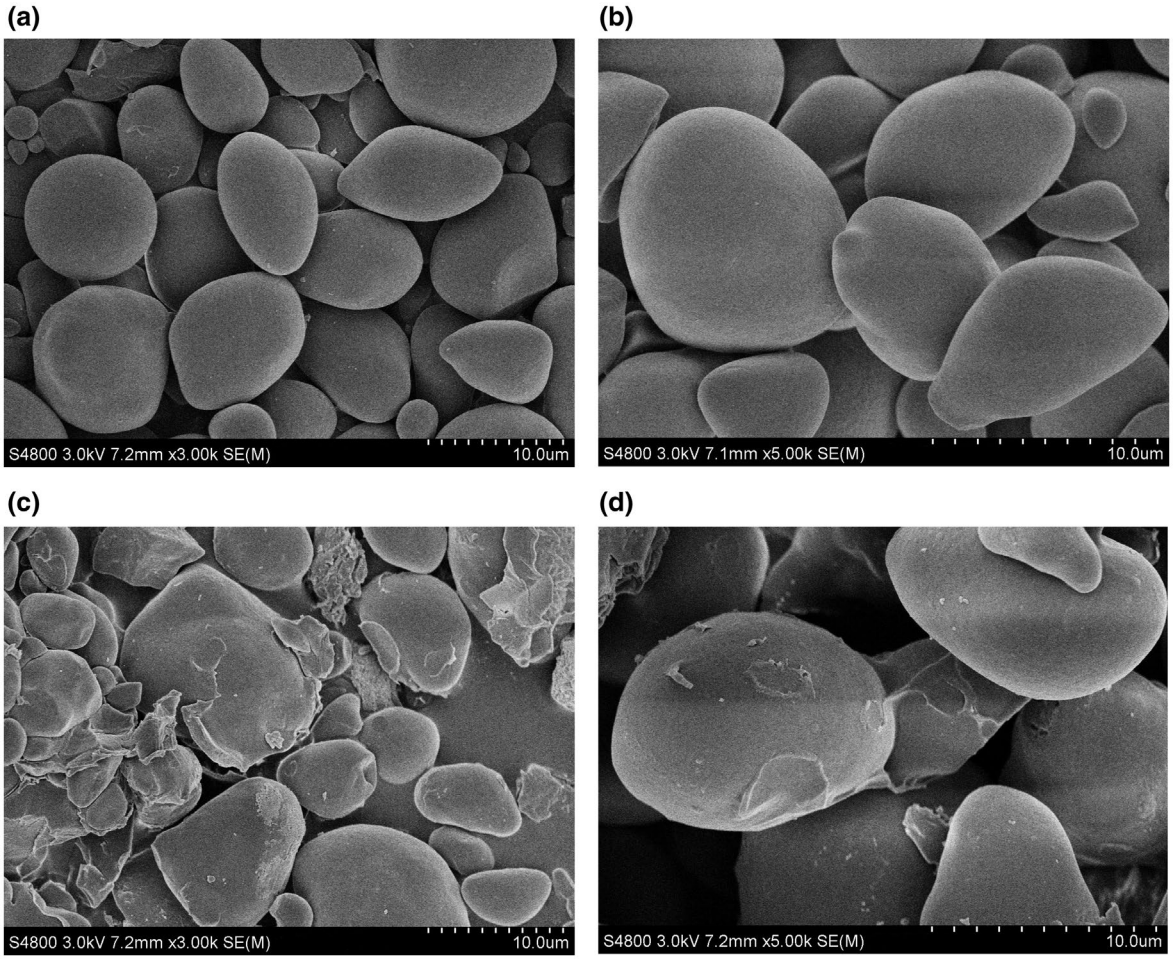

FIGURE 6 SEM analysis (magnification 3,000×, 5,000×) of CS (a,b) and CSA (c,d)

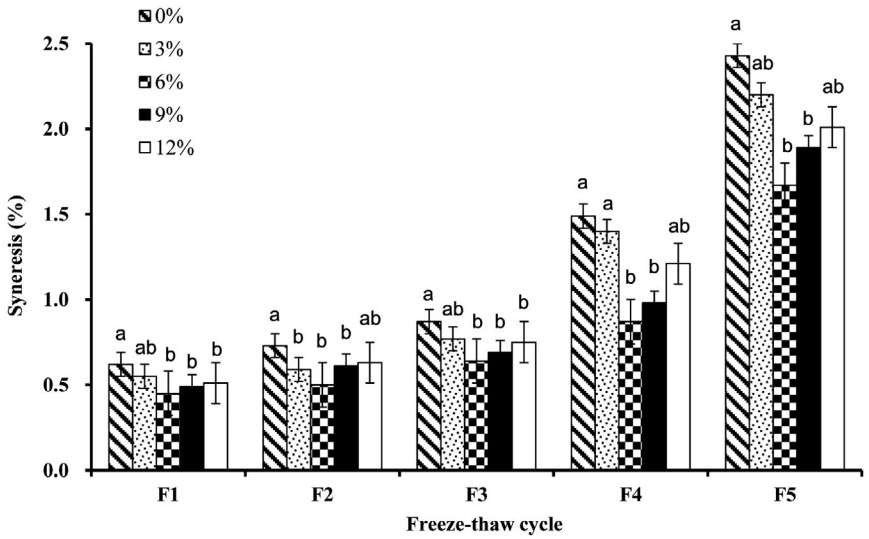

FIGURE 7 Syneresis of the dough samples upon varying the number of freeze-thaw cycles. All data were means of triplicate. Results are expressed as mean values ± *SD*. The Duncan's multiple range test was applied. Means in a column with same superscripts are not significantly different ($p < .05$)

3.7 | Texture characteristics analysis

It can be seen from Figure 8a that the amount of CSA in the dough affected the firmness of the freeze-thaw dough. The firmness of the dough was found to decrease initially and then increase with the addition of CSA. It was found to be lower relative to the initial firmness obtained for 0% CSA. The firmness of the dough was minimal for the CSA concentration of 6%. In principle, the CSA in the dough contains a large number of hydrophilic groups that easily absorb water and form a large cross-linking network, which promotes

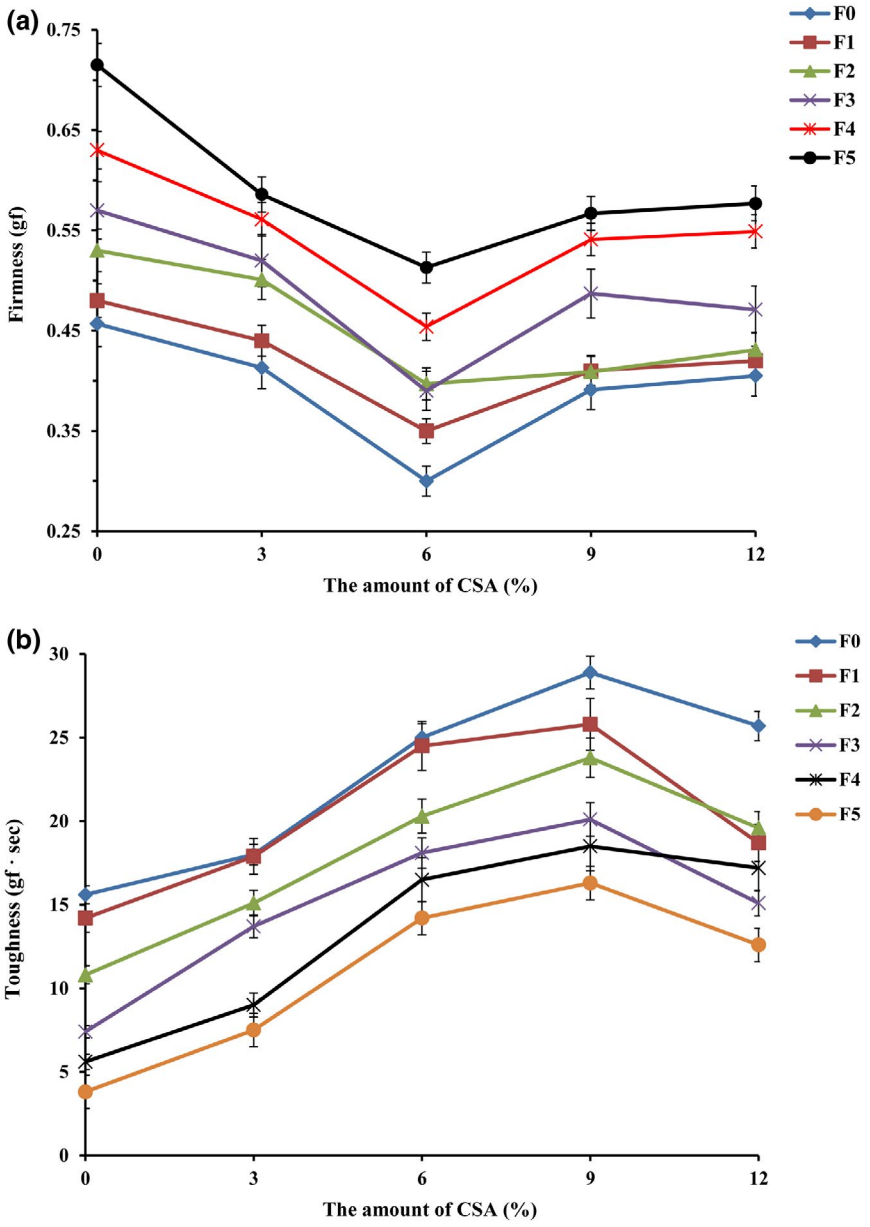

FIGURE 8 The effect of the amount of CSA in the dough on (a) the firmness and (b) the toughness of freeze-thaw dough

the starch and protein in the dough to penetrate with each other to form a polymer network (Tuankriangkrai & Benjakul, 2010). As a result, the firmness of the dough was reduced. However, there was an increase in the firmness as the amount of CSA exceeded 6%. This may be attributed to the redistribution of moisture in the dough. The firmness of the raw dough increased with the increase in the number of freeze-thaw cycles. This can be due to syneresis of the dough during the freeze-thaw cycles. The water continuously migrated and dissipated during the freezing and thawing processes. The moisture content of the dough decreased, which resulted in an increase in the firmness of the dough (Romero et al., 2017).

Figure 8b is a graphical representation of the influence of modified starch on the toughness of raw dough. With an increase in the addition of CSA, the toughness of the raw dough initially increased and then decreased continuously. The toughness was found to be the highest for the CSA concentration of 9%. This was attributed to the continuous increase in the amount of modified starch, which promoted the interpenetration of starch, protein, and other substances in the dough to form more complex polymer networks that inhibited the growth of ice crystals, thereby improving the toughness of the raw dough. On the other hand, the toughness of CSA gradually decreased with an increase in the number of freeze-thaw cycles. This is due to the continuous formation of ice crystals in the dough with the number of freeze-thaw cycles. The degree of damage to the gluten network structure was intensified, reducing the toughness of the dough (Kazemi & Zulkurnain, 2015). The textural properties were better for the CSA concentrations of 6%–9%.

4 | CONCLUSIONS

The CS molecules were modified using acetic anhydride. The structural properties of CSA and its effect on the water retention and texture properties of the dough were investigated. The processing conditions of CSA obtained from the response surface prediction modeling were reasonable and reliable. The apparent viscosity of CSA prepared under most conditions was 109.38% higher than that of the CS molecules. The FT-IR spectroscopy confirmed the introduction of acetyl groups on the CS molecules. The CS was found to have a C-type crystalline form after acetylation, which was confirmed by XRD. The SEM analysis showed dents, cracks, and wrinkles in some regions of the CSA granular surface. Moreover, the dough treated with CSA showed excellent water retention. The modified starch showed improved firmness and toughness of the frozen-thawed dough. To conclude, the optimization of the preparation process of CSA through response surface modeling may provide a new method for the utilization of discarded chestnuts in the food industry.

ACKNOWLEDGMENTS

The authors are grateful for the support of the Youth Fund Project of the Education Department, Hebei Province, China (QN2018030) and the Laboratory Construction and Asset Management Research Project of Higher Education Society, Hebei Province, China (sy202109).

CONFLICT OF INTEREST

The authors have declared no conflicts of interest for this article.

AUTHOR CONTRIBUTIONS

Na Hu: Software; Writing-original draft. **Luning Li:** Investigation; Methodology; Project administration.

DATA AVAILABILITY STATEMENT

The data that support the findings of this study are available from the corresponding author upon reasonable request.

ORCID

Na Hu https://orcid.org/0000-0002-2111-0378
Luning Li https://orcid.org/0000-0002-0104-3681

REFERENCES

Ahmed, J., & Al-Attar, H. (2015). Effect of drying method on rheological, thermal, and structural properties of chestnut flour doughs. *Food Hydrocolloids*, *51*, 76–87. https://doi.org/10.1016/j.foodhyd.2015.04.030

Asima, S., Masoodi, F. A., Gani, A., & Ashwar, B. A. (2017). Physicochemical, rheological and structural characterization of acetylated oat starches. *LWT - Food Science and Technology*, *80*, 19–26. https://doi.org/10.1016/j.lwt.2017.01.072

Attanasio, G., Cinquanta, L., Albanese, D., & Matteo, M. D. (2014). Effects of drying temperatures on physico-chemical properties of dried and rehydrated chestnuts (*Castanea sativa*). *Food Chemistry*, *88*, 583–590. https://doi.org/10.1016/j.foodchem.2004.01.071

Bao, W., Li, Q., Wu, Y., & Ouyang, J. (2018). Insights into the crystallinity and in vitro, digestibility of chestnut starch during thermal processing. *Food Chemistry*, *269*, 244–251. https://doi.org/10.1016/j.foodchem.2018.06.128

Chylińska, M., Szymańskachargot, M., & Zdunek, A. (2016). FT-IR and FT-Raman characterization of non-cellulosic polysaccharides fractions isolated from plant cell wall. *Carbohydrate Polymers*, *154*, 48–54. https://doi.org/10.1016/j.carbpol.2016.07.121

Colussi, R., Singh, J., Kaur, L., Zavareze, E. D. R., Dias, A. R. G., Stewart, R. B., & Singh, H. (2017). Microstructural characteristics and gastro-small intestinal digestion in vitro of potato starch: Effects of refrigerated storage and reheating in microwave. *Food Chemistry*, *226*, 171–178. https://doi.org/10.1016/j.foodchem.2017.01.048

Cuenca, P., Ferrero, S., & Albani, O. (2019). Preparation and characterization of cassava starch acetate with high substitution degree. *Food Hydrocolloids*, *2019*(100), 105430.

Diop, C. I. K., Li, H. L., Xie, B. J., & Shi, J. (2011). Effects of acetic acid/acetic anhydride ratios on the properties of corn starch acetates. *Food Chemistry*, *126*, 1662–1669. https://doi.org/10.1016/j.foodchem.2010.12.050

Fariña, M., Torres, M. D., & Moreira, R. (2019). Starch hydrogels from discarded chestnuts produced under different temperature-time gelatinisation conditions. *International Journal of Food Science and Technology*, *54*, 1179–1186. https://doi.org/10.1111/ijfs.14070

Galvão, A. M. M. T., Zambelli, R. A., Araújo, A. W. O., & Bastos, M. S. R. (2018). Edible coating based on modifified corn starch/tomato powder: Effffect on the quality of dough bread. *LWT–Food Science and Technology*, *89*, 518–524.

Hao, H. N., Li, Q., Bao, W., Wu, Y., & Ouyang, J. (2018). Relationship between physicochemical characteristics and in vitro digestibility of chestnut (*Castanea mollissima*) starch. *Food Hydrocolloids*, *84*, 193–199. https://doi.org/10.1016/j.foodhyd.2018.05.031

Hu, N., Gu, X., Li, L. N., Ouyang, J., Wang, F. J., Wang, J. Z., & Fan, Z. Y. (2014). Synthesis and evaluation of microstructure of physphorylated chestnut starch. *Journal of Food Process Engineering*, *37*, 75–85.

Hu, N., Li, L. N., Tang, E. J., & Liu, X. Y. (2020). Structural, physicochemical, textural, and thermal properties of phosphorylated chestnut starches with different degrees of substitution. *Journal of Food Processing and Preservation*, *44*, e14457. https://doi.org/10.1111/jfpp.14457

Jeddou, K. B., Chaari, F., Maktouf, S., Nouri-Ellouz, O., Helbert, C. B., & Ghorbel, R. E. (2016). Structural, functional, and antioxidant properties of water-soluble polysaccharides from potatoes peels. *Food Chemisty*, *205*, 97–105. https://doi.org/10.1016/j.foodchem.2016.02.108

Kamarudin, F., & Gan, C. Y. (2016). Molecular structure, chemical properties and biological activities of pinto bean pod polysaccharide. *International Journal of Biological Macromolecules*, *88*, 280–287. https://doi.org/10.1016/j.ijbiomac.2016.04.003

Kazemi, M., & Zulkurnain, M. (2015). Effect of partial replacement of corn flour with durian seed flour and pumpkin flour on cooking yield, texture properties, and sensory attributes of gluten free pasta. *LWT–Food Science and Technology*, *63*, 184–190.

Lin, D., Zhou, W., Yang, Z., Zhong, Y., Xing, B., Wu, Z., Chen, H., Wu, D., Zhang, Q., Qin, W., & Li, S. (2019). Study on physicochemical properties, digestive properties and application of acetylated starch in noodles. *International Journal of Biological Macromolecules*, *128*, 948–956. https://doi.org/10.1016/j.ijbiomac.2019.01.176

Liu, C., Wang, S., Chang, X., & Wang, S. (2015). Structural and functional properties of starches from Chinese chestnuts. *Food Hydrocolloids*, *43*, 568–576. https://doi.org/10.1016/j.foodhyd.2014.07.014

Mi, J., Liang, Y., Li, G. H., Tan, Z. P., & Cui, B. (2014). Influence of acetylated starch on the quality of quick-frozen dumplings. *Jiangsu Seasoning Food*, *139*, 27–29.

Molavi, H., Razavi, S. M. A., & Farhoosh, R. (2018). Impact of hydrothermal modifications on the physicochemical, morphology, crystallinity, pasting and thermal properties of a corn starch. *Food Chemistry*, *245*, 385–393. https://doi.org/10.1016/j.foodchem.2017.10.117

Motta Romero, H., Santra, D., Rose, D., & Zhang, Y. (2017). Dough rheological properties and texture of gluten-free pasta based on proso millet flour. *Journal of Cereal Science*, *74*, 238–243. https://doi.org/10.1016/j.jcs.2017.02.014

Oh, S. M., Choi, H. W., Kim, B. Y., & Baik, M. Y. (2017). Retrogradation kinetics of chestnut starches cultivated in three regions of Korea. *Food Science and Biotechnology*, *26*, 663–670. https://doi.org/10.1007/s10068-017-0103-5

Oh, S.-M., Kim, H.-Y., Bae, J.-E., Ye, S.-J., Kim, B.-Y., Choi, H. D., Choi, H.-W., & Baik, M.-Y. (2019). Physicochemical and retrogradation properties of modified chestnut starches. *Food Science and Biotechnology*, *28*, 1723–1731. https://doi.org/10.1007/s10068-019-00622-8

Pan, A., Dai, Y., Hou, H., Wang, W., Ding, X., Zhang, H., Li, X., & Dong, H. (2020). Preparation of acetylated starch by rolling-assisted method and its influence mechanism. *Journal of Food Measurement and Characterization*, *14*, 623–631. https://doi.org/10.1007/s11694-019-00308-z

Paulik, S., Yu, W. W., Flanagan, B., Gilbert, R. G., Jekle, M., & Becker, T. (2019). Characterizing the impact of starch and gluten-induced alterations on gelatinization behavior of physically modified model dough. *Food Chemistry*, *301*, 125276. https://doi.org/10.1016/j.foodchem.2019.125276

Przetaczek-Rożnowska, I. (2017). Physicochemical properties of starches isolated from pumpkin compared with potato and corn starches. *International Journal of Biological Macromolecules*, *101*, 536–542. https://doi.org/10.1016/j.ijbiomac.2017.03.092

Sukhija, S., Singh, S., & Riar, C. S. (2016). Physicochemical, crystalline, morphological, pasting and thermal properties of modified lotus rhizome (*Nelumbo nucifera*) starch. *Food Hydrocolloids*, *60*, 50–58. https://doi.org/10.1016/j.foodhyd.2016.03.013

Sun, S. L., Zhang, G. W., & Ma, C. Y. (2016). Preparation, physicochemical characterization and application of acetylated lotus rhizome starches. *Carbohydrate Polymers*, *135*, 10–17. https://doi.org/10.1016/j.carbpol.2015.07.090

Suvakanta, D., Narsimha, M. P., Pulak, D., Joshabir, C., & Biswajit, D. (2014). Optimization and characterization of purified polysaccharide from *Musa sapientum* L. as a pharmaceutical excipient. *Food Chemistry*, *149*, 76–83. https://doi.org/10.1016/j.foodchem.2013.10.068

Tang, M. Y., Hou, F., Wu, Y. W., Liu, Y. G., & Ouyang, J. (2019). Purification, characterization and tyrosinase inhibition activity of polysaccharides from chestnut (*Castanea mollissima* Bl.) kernel. *International Journal of Biological Macromolecules*, *131*, 309–314. https://doi.org/10.1016/j.ijbiomac.2019.03.065

Tuankriangkrai, S., & Benjakul, S. (2010). Effect of modified tapioca starch on the stability of fish mince gels subjected to multiple freeze thawing. *Journal of Muscle Foods*, *21*, 399–416. https://doi.org/10.1111/j.1745-4573.2009.00190.x

Volket, B., Lehman, A., Greco, T., & Nejad, M. H. (2010). A comparison of different synthesis routes for starch acetates and the resulting mechanical properties. *Carbohydrate Polymers*, *79*, 571–577. https://doi.org/10.1016/j.carbpol.2009.09.005

Wang, M., Sun, M. Q., Zhang, Y. Y., Chen, Y., Wu, Y. W., & Ouyang, J. (2019). Effect of microwave irradiation-retrogradation treatment on the digestive and physicochemical properties of starches with different crystallinity. *Food Chemistry*, *298*, 125015. https://doi.org/10.1016/j.foodchem.2019.125015

Wang, Y. N., Hou, Z. H., & Tan, Z. P. (2017). Effect of modified starch on baking properties of frozen dough bread. *Cereals and Oils*, *30*, 81–83.

Xiao, H., Yang, T., Lin, Q., Liu, G.-Q., Zhang, L., Yu, F., & Chen, Y. (2016). Acetylated starch nanocrystals: Preparation and antitumor drug delivery study. *International Journal of Biological Macromolecules*, *89*, 456–464. https://doi.org/10.1016/j.ijbiomac.2016.04.037

Xu, Y., Ding, W. Q., Liu, J., Li, Y., Kennedy, J. F., Gu, Q., & Shao, S. X. (2010). Preparation and characterization of organic-soluble acetylated starch nanocrystals. *Carbohydrate Polymers*, *80*, 1078–1084. https://doi.org/10.1016/j.carbpol.2010.01.027

Yu, S., Liu, J., Yang, Y., Ren, J., Zheng, X., & Kopparapu, N. K. (2016). Effects of amylose content on the physicochemical properties of Chinese chestnut starch. *Starch-Stärke*, *68*, 112–118. https://doi.org/10.1002/star.201500177

Zhang, K. L., Dai, Y. Y., Hou, H. X., Li, X. Y., Dong, H. Z., Wang, W. T., & Zhang, H. (2018). Preparation of high quality starch acetate under grinding and its influence mechanism. *International Journal of Biological Macromolecules*, *120*, 2026–2034. https://doi.org/10.1016/j.ijbiomac.2018.09.196

Zhang, Y. Y., Li, G. P., Wu, Y. W., Yang, Z. L., & Ouyang, J. (2019). Influence of amylose on the pasting and gel texture properties of chestnut starch during thermal processing. *Food Chemistry*, *294*, 378–383. https://doi.org/10.1016/j.foodchem.2019.05.070

Zhao, J. K., Zhang, Y. Y., Wu, Y. W., Liu, L. L., & Ouyang, J. (2018). Physicochemical properties and in vitro digestibility of starch from naturally air-dried chestnut. *International Journal of Biological Macromolecules*, *117*, 1074–1080. https://doi.org/10.1016/j.ijbiomac.2018.06.034

Ziobro, R., Korus, J., Witczak, M., & Juszczak, L. (2012). Influence of modified starches on properties of gluten-free dough and bread. Part II: Quality and staling of gluten-free bread. *Food Hydrocolloids*, *29*, 68–74.

How to cite this article: Hu N, Li L. Optimization of chestnut starch acetate synthesis by response surface methodology and its effect on dough properties. *J Food Process Preserv.* 2021;00:e15431. https://doi.org/10.1111/jfpp.15431